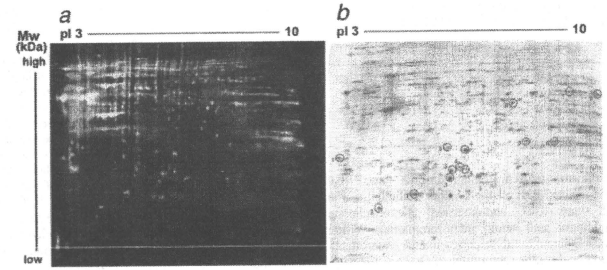


FIGURE 1 – Proteomic analysis of OVISE CCC and OVSAHO SAC cell lines. Representative gel images of 3 independent experiments are shown. A 2D-DIGE gel image of OVISE CCC and OVSAHO SAC cell lines is shown in (*a*). Green spots correspond to proteins upregulated in OVISE cells (Cy3 labeled) compared with OVSAHO cells (Cy5 labeled). Red spots correspond to proteins upregulated in OVSAHO cells (Cy5 labeled) compared with OVISE cells (Cy3 labeled). Yellow spots correspond to proteins expressed at the same level in the OVISE and OVSAHO cell lines. A corresponding silver stain gel image is shown in (*b*).

Japan) in a hot water bath at 98°C for 40 min. In brief, quenching endogenous peroxidase with 3% $H_2O_2$ in methanol for 20 min. After treatment with BlockAce (Dainippon Sumitomo Pharmaceutical, Osaka, Japan) for 30 min at room temperature, the sections were incubated with a goat polyclonal anti-Anx A4 antibody at 1:100 dilution at 4°C overnight and subsequently incubated with a biotinylated anti-goat IgG antibody (Vector Laboratories Inc.) at room temperature for 1 hr. The antibody complex was detected by incubation with an avidin-biotin-peroxidase complex solution (Vector Laboratories Inc.) and visualized with 3.3′-diaminobenzidine tetrahydrochloride (MERCK, Darmstadt, Germany). Tissue sections were counter-stained with hematoxylin. Three gynecologic oncologists (A.K., T.M., Y.U.), blinded to the histological data, reviewed the stained sections. Cases with >90% of tumor cells staining positively with the anti-Anx A4 antibody were considered strongly positive (+++), cases with >50% but <90% Anx A4-positive cells medium positive (++), those with <50% positive cells weakly positive (+) and those with no or hardly any positive cells were considered negative.

*Construction of Anx A4 expression vector*

Total RNA from OVISE cells was purified with an RNA-Bee solution (Tel-Test Inc., Friendswood, TX) and cDNA was prepared with a SuperScript™ III Reverse Transcriptase Kit (Invitrogen). To construct the Anx A4 expression vector, cDNA of human Anx A4 was amplified using KOD-plus (Toyobo Co. Ltd., Osaka, Japan) with the following primers: Anx A4 forward primer 5′-ttgacctagagtcatggcca-3′ and Anx A4 reverse primer 5′-tttaatcatctcctccacag-3′. The amplified cDNA was then inserted into pcDNA3.1/V5-His-TOPO vector (Invitrogen) and designated pcDNA3.1-Anx A4. The DNA sequence of Anx A4 cDNA inserted into the plasmid was confirmed using the ABI PRISM 3100 Genetic Analyzer (Applied Biosystems, Foster City, USA).

*Generation of Anx A4 stable transfectant cells*

To generate Anx A4 stable transfectant cells, the OVSAHO cell line was transfected with pcDNA3.1-Anx A4 using Lipofectamine 2000 (Invitrogen) according to the manufacturers' instructions, after which the cells were selected with 500 μg/ml of Geneticin (GIBCO, Invitrogen, Carlsbad, CA). We also transfected empty vector into the OVSAHO cell line using the same procedure described earlier to generate control cells. Stable clones were maintained in 250 μg/ml of Geneticin. Western blot analysis was performed to confirm the levels of Anx A4 expression in Anx A4 transfectant cells and empty vector control cells.

*Measurement of $IC_{50}$ values after carboplatin treatment*

Anx A4 transfected OVSAHO cells and empty vector control cells were seeded in 96-well plates (3,000 cells/well) (Costar; Corning Inc., Corning, NY) for 24 hr and then exposed to various concentrations (0-150 μM) of carboplatin for 72 hr. The cells were incubated with 10 μl of Cell Counting Kit-8 (Dojindo, Osaka, Japan) in 100 μl RPMI-1640 medium for 3 hr. Absorbance at 450 nm was measured with a microplate reader (Bio-Rad Model 680), and absorbance values were expressed as percentages relative to those for untreated controls, and the concentrations resulting in 50% inhibition of cell growth ($IC_{50}$ values) were calculated.

*Measurement of intracellular platinum accumulation*

Carboplatin accumulation in Anx A4 transfected cells and control cells was analyzed according to a previously established method[17] with minor modifications. In brief, $1.5 \times 10^6$ cells were seeded into a 60-mm tissue culture dish and incubated for 24 hr. The cells were then exposed to 2 mM carboplatin for 60 min at 37°C and washed twice with PBS either immediately or after 360 min of incubation in carboplatin-free RPMI 1640 medium supplemented with 10% FBS (HyClone Laboratories). After whole-cell extracts were prepared, the concentration of intracellular platinum was determined by using a polarized Zeeman atomic absorption spectrophotometer (model Z-8000; Hitachi, Ltd., Tokyo, Japan). The absolute concentration of platinum in each sample was determined from a calibration curve prepared with a platinum standard solution.

*Statistical analysis*

Student's *t* tests were used for statistical analyses. For the immunohistochemical analysis, a nonparametric analysis (the Kruskal–Wallis test) was used. A value of $p < 0.05$ was considered statistically significant.

## Results

*Anx A4 expression is elevated in CCC cell lines compared with SAC cell lines*

The protein expression profiles of OVISE (CCC) and OVSAHO (SAC) cell lines were compared by means of 2D-DIGE analyses using fluorminimal dye-labeled protein extracts. The resulting gel images and corresponding silver-stained gels are shown in Figures 1*a* and 1*b*. Eight proteins highly expressed in OVISE cells and 6 proteins in OVSAHO cells were selected for identification by LC-MS/MS analysis. The results of these analyses (Table II) revealed

TABLE II – PROTEINS DIFFERENTIALLY EXPRESSED IN OVISE AND OVSAHO CELL LINES

| Spot no. | Access. no. | Identified protein | $M_w$ (Da) | pI | Coverage (%) |
|---|---|---|---|---|---|
| *Proteins upregulated in OVISE cells compared with OVSAHO cells* | | | | | |
| 1 | P09211 | Glutathione S-transferase P | 23,438 | 5.44 | 38 |
| 2 | P09525 | Annexin A4 (Annexin IV) | 35,957 | 5.85 | 49 |
| 3 | P04792 | Heat-shock protein beta-1 | 22,826 | 5.98 | 39 |
| 4 | Q13011 | Delta3,5-delta2,4-dienoyl-CoA isomerase, mitochondrial precursor | 36,136 | 8.16 | 28 |
| 5 | P30040 | Endoplasmic reticulum protein ERp29 precursor | 29,032 | 6.77 | 15 |
| 6 | O75874 | Isocitrate dehydrogenase [NADP] cytoplasmic | 46,915 | 6.53 | 39 |
| 7 | P68104 | Elongation factor 1-alpha 1 | 50,451 | 9.1 | 14 |
| 8 | P68104 | Elongation factor 1-alpha 1 | 50,451 | 9.1 | 19 |
| *Proteins upregulated in OVSAHO cells compared with OVISE cells* | | | | | |
| 1 | Q07021 | Complement component 1 Q subcomponent-binding protein, mitochondrial precursor | 31,742 | 4.74 | 14 |
| 2 | O75947 | ATP synthase D chain, mitochondrial | 18,405 | 5.22 | 41 |
| 3 | P30084 | Enoyl-CoA hydratase, mitochondrial precursor | 31,823 | 8.34 | 27 |
| 4 | P42126 | 3,2-trans-enoyl-CoA isomerase, mitochondrial precursor | 33,080 | 8.8 | 10 |
| 5 | P45880 | Voltage-dependent anion-selective channel protein 2 | 38,639 | 6.32 | 25 |
| 6 | P45880 | Voltage-dependent anion-selective channel protein 2 | 38,639 | 6.32 | 25 |

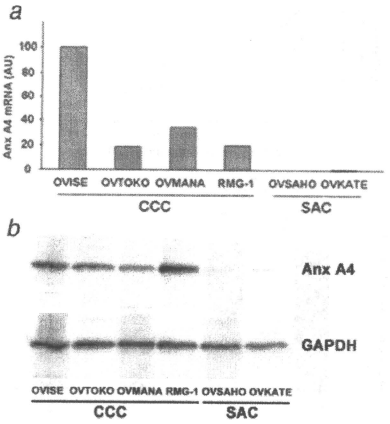


FIGURE 2 – Real-time RT-PCR and Western blot analysis of levels of Annexin A4 expression in ovarian cancer cell lines. Levels of Annexin A4 mRNA in ovarian CCC cell lines (OVISE, OVTOKO, OVMANA and RMG-1) and in ovarian SAC cell lines (OVSAHO and OVKATE) were determined by real-time RT-PCR (*a*). Levels of Annexin A4 protein in ovarian CCC cell lines (OVISE, OVTOKO, OVMANA and RMG-1) and in ovarian SAC cell lines (OVSAHO and OVKATE) were determined by Western blot analysis (*b*).

enhanced expression of the Anx A4 protein in the OVISE cell line compared with the OVSAHO cell line.

The specific overexpression of Anx A4 in ovarian CCC cell lines compared with that in SAC cell lines was further evaluated by real-time RT-PCR (Fig. 2*a*) and Western blot analysis (Fig. 2*b*). As shown in Figure 2*a*, expression of Anx A4 (mRNA level) in OVISE, OVTOKO, OVMANA and RMG-1 (CCC) cell lines was enhanced compared with the OVSAHO and OVKATE (SAC) cell lines where Anx A4 expression (mRNA level) was barely detectable. Western blot analysis (Fig. 2*b*) also demonstrated enhanced expression of Anx A4 (protein level) in OVISE, OVTOKO, OVMANA, RMG-1 (CCC) cell lines compared with the OVSAHO and OVKATE (SAC) cell lines.

### *Enhanced expression of Anx A4 protein in tumors of ovarian CCC patients*

Next, we determined whether levels of Anx A4 protein are elevated in tumors of patients with ovarian CCC compared with other ovarian cancers. For this analysis, we performed an immunohistochemical study of Anx A4 expression in tumor tissue samples from a large cohort of ovarian cancer patients (126 patients in total). In addition, we performed Western blot analysis using several frozen tumor tissue samples and compared the results with those of the immunohistochemical study. Representative immunohistochemical staining of Anx A4 in tissue sections from patients with ovarian cancer revealed intense Anx A4 staining in ovarian CCC compared with other histological types (Fig. 3*a*). Positive staining scores for Anx A4 in tissue sections from patients with other types of ovarian cancers are shown in Figure 3*b*. We observed significantly stronger ($p < 0.01$) positive staining in tissue sections from patients with ovarian CCC compared with patients with ovarian endometrioid and serous adenocarcinoma. Of 43 CCC tissue sections, more than 30 were strongly positive for Anx A4 (+++) compared with only 5 of the 62 SAC samples. Western blot analysis showed enhanced expression of Anx A4 in CCC tumor samples that had demonstrated strong Anx A4 immunohistochemical staining (+++) but barely detectable expression of Anx A4 in SAC tumor samples that had demonstrated negative (−) Anx A4 immunohistochemical staining (Fig. 3*c*).

### *Transfection of Anx A4 cDNA into ovarian cancer cells enhances resistance to carboplatin treatment and modulates drug cellular efflux*

Because Anx A4 has been demonstrated to perform a functional role in chemoresistance in some cancer cell lines,[14] we determined whether Anx A4 can also confer chemoresistance to epithelial ovarian cancer cells. For this study, we generated Anx A4 stably transfected OVSAHO cells. Figure 4*a* shows a Western blot analysis of Anx A4 levels in OVSAHO parent cells, Anx A4 stably transfected OVSAHO cells and empty vector transfected control cells. Figure 4*b* shows cell survival plots for control and OVSAHO/Anx A4 cell lines after treatment with increasing concentrations of carboplatin (0–150 μM). From this analysis, we determined the $IC_{50}$ carboplatin concentration values for the 2 cell lines. Higher (approximately double) $IC_{50}$ carboplatin concentration was observed in the OVSAHO/Anx A4 ($IC_{50}$ = 42 μM) cells compared with the empty vector control cells ($IC_{50}$ = 23 μM). These results demonstrate that Anx A4 can confer chemoresist-

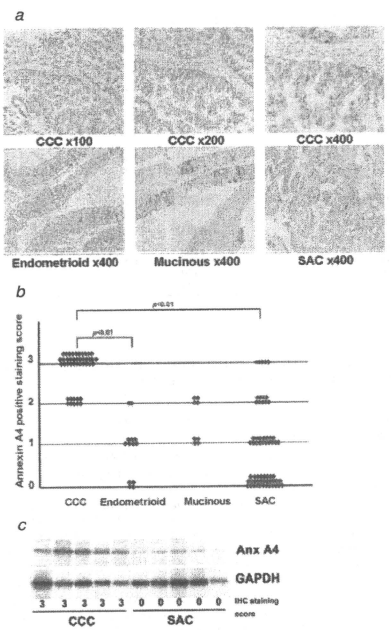


FIGURE 3 – Immunohistochemical analysis of Annexin A4 in ovarian cancer tumors. Levels of Annexin A4 protein in 126 epithelial ovarian cancer samples were determined by immunohistochemical analysis. Representative images of tissue sections from CCC ($n = 43$), endometrioid ($n = 8$), mucinous ($n = 13$) and serous adenocarcinoma ($n = 62$) ovarian cancer patients after immunohistochemical staining for Annexin A4 (*a*). Annexin A4-positive staining scores of tissue sections from ovarian cancer tumors (*b*). The *p* value between CCC and SAC is provided as determined by the nonparametric Kruskal–Wallis test. Western blot analysis using 5 CCC frozen tumor samples and 5 SAC frozen tumor samples (*c*).

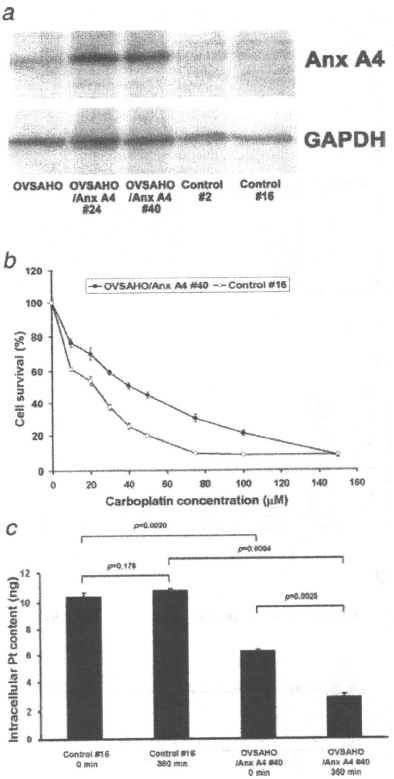


FIGURE 4 – Transfection of Annexin A4 cDNA into ovarian cancer cells confers resistance to carboplatin and decreases intracellular Pt accumulation. Cell survival (expressed as a percentage relative to control untreated cells) after 72 hr treatment of OVSAHO/Anx A4 and empty vector control cells with different concentrations of carboplatin (Figure 4*a*). The obtained IC50 values were 42 μM for OVSAHO/Anx A4 no. 40 and 23 μM for Control no. 16 (not shown in figure). Intracellular platinum content after treatment with 2 mM carboplatin for 60 min with or without after 360 min of incubation in carboplatin-free medium in OVSAHO/Anx A4 cells and control cells, as determined by atomic absorption spectrophotometry (Figure 4*c*).

ance in ovarian cancer cells. To investigate the molecular mechanisms of chemoresistance induced by Anx A4, we quantitated the intracellular platinum content after treatment of OVSAHO/Anx A4 and empty vector control cells with carboplatin. Figure 4*c* shows an analysis of intracellular platinum accumulation in OVSAHO/Anx A4 cells and empty vector control cells after carboplatin treatment with or without an additional incubation time (360 min) in carboplatin-free medium. Significantly ($p = 0.0020$) reduced levels of intracellular platinum accumulation were noted in OVSAHO/Anx A4 cells (OVSAHO/Anx A4 no. 40, 0 min) compared with empty vector control cells (Control no. 16, 0 min) when neither cell line underwent additional incubation in carboplatin-free medium. Control cells displayed no significant difference ($p = 0.178$) in intracellular platinum content between 0 min and 360 min of additional carboplatin-free incubation time (Control no. 16, 0 min *vs.* Control no. 16, 360 min), whereas OVSAHO/Anx A4 cells showed a significant decrease ($p = 0.0025$) in intracellular platinum content at 360 min as compared with at 0 min of additional carboplatin-free incubation time (OVSAHO/Anx A4 no. 40, 0 min *vs.* OVSAHO/Anx A4 no. 40, 360 min). Furthermore, OVSAHO/Anx A4 cells displayed significantly decreased ($p = 0.0004$) levels of intracellular platinum con-

tent compared with control cells after an additional 360 min of carboplatin-free incubation (Control no. 16, 360 min *vs.* OVSAHO/Anx A4 no. 40, 360 min), which suggests a role for Anx A4 in enhancing cellular platinum efflux.

## Discussion

The use of carboplatin and paclitaxel for the treatment of ovarian cancers has significantly improved survival rates in patients with this disease.[18] However, of the 4 major histological types of ovarian cancer, CCC of the ovary is characterized by strong chemoresistance.[2] Consequently, patients with this disease are associated with significantly lower 5-year survival rates than patients with other histological types of ovarian cancer.[19,20] However, the molecular mechanisms of chemoresistance in this disease have remained poorly understood. Thus, the identification of proteins which are involved in chemoresistance in ovarian CCC is of major clinical importance because these proteins may constitute novel therapeutic targets in this disease.

In this study, we performed a 2D-DIGE proteomic analysis using ovarian cancer cell lines for the identification of a candidate protein associated with chemoresistance in ovarian CCC. We identified 8 proteins differentially upregulated in OVISE CCC cells compared with OVSAHO SAC cells (Table II). From among those 8 proteins, we focused on Anx A4, a calcium-dependent phospholipid-binding protein, which is localized proximal to the cell membrane and plays an important role in membrane fluidity or trafficking.[10]

We confirmed by means of both real-time RT-PCR (mRNA levels) and Western blot analysis (protein levels) that expression of Anx A4 was significantly enhanced in ovarian CCC cell lines compared with in non-CCC ovarian cancer cell lines (Figs. 2*a* and 2*b*). The findings of our analysis using ovarian cancer cell lines are in agreement with those of the proteomic study of Morita *et al.*,[15] in which Anx A4 was identified as being differentially upregulated in ovarian CCC cell lines (OVISE and OVTOKO) compared with an ovarian mucinous cancer cell line.

Previous studies have associated Anx A4 protein with chemoresistance. For example, in a study of Han *et al.*,[14] Anx A4 was observed to be elevated in a paclitaxel-resistant human lung cancer cell line and transfection of Anx A4 cDNA into embryonic kidney 293T cells to confer resistance to paclitaxel. Because Anx A4 has been shown to be involved in modulating membrane permeability and membrane trafficking,[10] it is conceivable that this involvement may result in modulation of both cellular drug influx and efflux after chemo-drug treatment. Taken together, these studies suggest that the strong chemoresistance characteristic of human ovarian CCC may be due to enhanced expression of Anx A4. However, it remained unclear whether levels of Anx A4 protein are significantly elevated in tumors of patients with ovarian CCC compared with other histological types.

In the study reported here, we, therefore, performed an immunohistochemical analysis of Anx A4 in tumor tissue samples from 126 patients with epithelial ovarian cancer to determine whether levels of Anx A4 protein are elevated in tumors of patients with ovarian CCC compared with other epithelial ovarian cancers. Because treatment with paclitaxel can enhance Anx A4 expression in cultured cells,[14] all patients examined in this analysis had undergone preliminary diagnosis and had not received chemotherapy (including carboplatin or paclitaxel) before surgery. The results of this analysis revealed significantly ($p < 0.01$) strong positive staining (enhanced expression) of Anx A4 in tumor tissue samples from patients with ovarian CCC compared with endometrioid and serous adenocarcinoma, which are known to represent chemosensitive histological types (Fig. 3*b*). Western blot analysis using frozen tumor samples were compatible with results of the IHC study (Fig. 3*c*). Thus, our study was able to demonstrate the presence of enhanced expression of Anx A4 in tumors of patients with ovarian CCC. This finding is in agreement with that of our proteomic analysis using ovarian cancer cell lines and indicates that Anx A4 may play a role in tumor resistance to cancer chemotherapy in patients with ovarian CCC.

To investigate a relationship between levels of expression of Anx A4 and patient prognosis, we reviewed clinical outcomes (recurrence, progression-free survival, etc.) of the 62 SAC patients including 5 patients with strong (+++)Anx A4 povitive staining in IHC analysis. Among the 5 SAC patients with high levels of Anx A4 expression, 2 patients are well and alive with no recurrence, whereas the other 2 patients have recurred within 1 or 2 years after treatment and 1 patient was out of follow-up. We have compared the progression-free survival between these 5 patients and Anx A4 negative SAC patients and there was no statistically significant difference between the 2 groups. Because the number of Anx A4-positive SAC patients is small, further investigation will be necessary in a larger cohort of patients.

Although previous studies have demonstrated a role for Anx A4 in conferring chemoresistance to human cancer cell lines,[14] a similar role in human epithelial ovarian cancer cells was not identified, and the specific mechanism of chemoresistance that Anx A4 confers was not previously determined. Therefore, we first studied cell survival after carboplatin treatment to confirm whether Anx A4 can enhance chemoresistance in epithelial ovarian cancer cells. We were unable to reduce Anx A4 protein levels in the OVISE CCC cell line, despite using various strategies (including siRNA), which may be due to the reported long half-life of Anx A4 protein (approximately 4 days).[21] We then tested the effect of forced overexpression of Anx A4 in the OVSAHO non-CCC (SAC) ovarian cancer cell line in which Anx A4 is not endogenously expressed. We observed enhanced chemoresistance to carboplatin treatment in cells that stably expressed Anx A4 compared with empty vector control cells (Figs. 4*a* and 4*b*). Thus, our results demonstrate that Anx A4 protein plays a role in the enhancement of chemoresistance in epithelial ovarian cancer cells.

We next examined intracellular platinum accumulation in both Anx A4 expressing ovarian cancer cells (OVSAHO/Anx A4 cells) and empty vector control cells after carboplatin treatment (Fig. 4*c*). Our results of carboplatin treatment with no carboplatin-free incubation revealed significantly reduced levels of intracellular platinum content in OVSAHO/Anx A4 cells compared with control cells, which indicates that Anx A4 inhibits cellular platinum influx and/or promotes cellular platinum efflux. Comparison of the results for 0 and 360 min carboplatin-free incubation showed that OVSAHO/Anx A4 cells are more active in promoting cellular platinum efflux compared with control cells. Taken together, these results demonstrate that Anx A4 plays a part in the enhancement of cellular platinum efflux.

Our study has demonstrated for the first time elevated levels of Anx A4 protein in patients with ovarian CCC and an association between elevated Anx A4 levels and enhanced chemoresistance to carboplatin in human epithelial ovarian cancer cells. It has also found evidence for the first time that Anx A4 confers chemoresistance in part by enhancing drug efflux. Thus, it is conceivable that the observed strong resistance to cancer chemotherapy (including carboplatin) specific to ovarian CCC tumors, compared with that of other epithelial ovarian tumors, is mediated through the enhanced expression of Anx A4 in patients with this disease. Therefore, Anx A4 may constitute a novel therapeutic target for overcoming resistance to cancer chemotherapy in patients with ovarian CCC. In view of the reported half-life of Anx A4 protein, such a therapeutic strategy is likely to involve the inhibition of the function rather than of the expression of Anx A4 in patients with CCC.

### Acknowledgements

The authors are grateful for experimental assistance from Ms. Y. Matsukawa and for secretarial assistance from Ms. Y. Ito and Ms. N. Kawakami.

## References


1. Jemal A, Siegel R, Ward E, Hao Y, Xu J, Murray T, Thun MJ. Cancer statistics, 2008. CA Cancer J Clin 2008;58:71–96.
2. Itamochi H, Kigawa J, Terakawa N. Mechanisms of chemoresistance and poor prognosis in ovarian clear cell carcinoma. Cancer Sci 2008; 99:653–8.
3. Jacobs IJ, Menon U. Progress and challenges in screening for early detection of ovarian cancer. Mol Cell Proteomics 2004;3:355–66.
4. Rapkiewicz AV, Espina V, Petricoin EF, III, Liotta LA. Biomarkers of ovarian tumours. Eur J Cancer 2004;40:2604–12.
5. Sugiyama T, Kamura T, Kigawa J, Terakawa N, Kikuchi Y, Kita T, Suzuki M, Sato I, Taguchi K. Clinical characteristics of clear cell carcinoma of the ovary: a distinct histologic type with poor prognosis and resistance to platinum-based chemotherapy. Cancer 2000;88: 2584–9.
6. Pectasides D, Pectasides E, Psyrri A, Economopoulos T. Treatment issues in clear cell carcinoma of the ovary: a different entity? Oncologist 2006;11:1089–94.
7. Kaetzel MA, Hazarika P, Dedman JR. Differential tissue expression of three 35-kDa annexin calcium-dependent phospholipid-binding proteins. J Biol Chem 1989;264:14463–70.
8. Zanotti G, Malpeli G, Gliubich F, Folli C, Stoppini M, Olivi L, Savoia A, Berni R. Structure of the trigonal crystal form of bovine annexin IV. Biochem J 1998;329:101–6.
9. Kaetzel MA, Mo YD, Mealy TR, Campos B, Bergsma-Schutter W, Brisson A, Dedman JR, Seaton BA. Phosphorylation mutants elucidate the mechanism of annexin IV-mediated membrane aggregation. Biochemistry 2001;40:4192–9.
10. Hill WG, Kaetzel MA, Kishore BK, Dedman JR, Zeidel ML. Annexin A4 reduces water and proton permeability of model membranes but does not alter aquaporin 2-mediated water transport in isolated endosomes. J Gen Physiol 2003;121:413–25.
11. Sohma H, Creutz CE, Gasa S, Ohkawa H, Akino T, Kuroki Y. Differential lipid specificities of the repeated domains of annexin IV. Biochim Biophys Acta 2001;1546:205–15.
12. Piljic A, Schultz C. Annexin A4 self-association modulates general membrane protein mobility in living cells. Mol Biol Cell 2006;17: 3318–28.
13. Kaetzel MA, Chan HC, Dubinsky WP, Dedman JR, Nelson DJ. A role for annexin IV in epithelial cell function. Inhibition of calcium-activated chloride conductance. J Biol Chem 1994;269:5297–302.
14. Han EK, Tahir SK, Cherian SP, Collins N, Ng SC. Modulation of paclitaxel resistance by annexin IV in human cancer cell lines. Br J Cancer 2000;83:83–8.
15. Morita A, Miyagi E, Yasumitsu H, Kawasaki H, Hirano H, Hirahara F. Proteomic search for potential diagnostic markers and therapeutic targets for ovarian clear cell adenocarcinoma. Proteomics 2006;6: 5880–90.
16. Shevchenko A, Wilm M, Vorm O, Mann M. Mass spectrometric sequencing of proteins silver-stained polyacrylamide gels. Anal Chem 1996;68:850–8.
17. Ikuta K, Takemura K, Sasaki K, Kihara M, Nishimura M, Ueda N, Naito S, Lee E, Shimizu E, Yamauchi A. Expression of multidrug resistance proteins and accumulation of cisplatin in human non-small cell lung cancer cells. Biol Pharm Bull 2005;28:707–12.
18. Paclitaxel plus carboplatin versus standard chemotherapy with either single-agent carboplatin or cyclophosphamide, doxorubicin, and cisplatin in women with ovarian cancer: the ICON3 randomised trial. Lancet 2002;360:505–15.
19. Tammela J, Geisler JP, Eskew PN, Jr, Geisler HE. Clear cell carcinoma of the ovary: poor prognosis compared to serous carcinoma. Eur J Gynaecol Oncol 1998;19:438–40.
20. O'Brien ME, Schofield JB, Tan S, Fryatt I, Fisher C, Wiltshaw E. Clear cell epithelial ovarian cancer (mesonephroid): bad prognosis only in early stages. Gynecol Oncol 1993;49:250–4.
21. Raynal P, Pollard HB, Srivastava M Cell cycle and post-transcriptional regulation of annexin expression in IMR-90 human fibroblasts. Biochem J 1997;322:365–71.

J Artif Organs (2009) 12:123–130
DOI 10.1007/s10047-009-0455-6



ORIGINAL ARTICLE

**Hanayuki Okura, MS · Hiroshi Komoda, MD, PhD**
**Yuichi Fumimoto, MD · Chun-Man Lee, MD, PhD**
**Toshirou Nishida, MD, PhD · Yoshiki Sawa, MD, PhD**
**Akifumi Matsuyama, MD, PhD**

# Transdifferentiation of human adipose tissue-derived stromal cells into insulin-producing clusters

**Abstract** Type 1 diabetes mellitus is caused by autoimmune destruction of insulin-producing beta cells. The major obstacle to transplantation of insulin-producing cells to cure the disease is the limited source of these cells. To overcome this problem, we describe here a multistep protocol for generation of insulin-producing islet-like clusters from human adipose tissue-derived stromal cells (ADSCs). Analysis using reverse transcription polymerase chain reaction detected enhanced expression of various pancreatic genes during the differentiation of ADSCs. Immunofluorescence analysis revealed functional similarities between cells derived from ADSCs and pancreatic islet cells, i.e., the presence of insulin- and C-peptide-coexpressing cells in the clusters and glucagon expression on the cell surface. The glucose challenge tests revealed the production of insulin, and such production was regulated via physiological signaling pathways. Our insulin-producing cells derived from ADSCs could be potentially used for cell therapy of type 1 diabetes mellitus.

**Key words** Diabetes mellitus · Adipose tissue-derived stromal cells · Insulin · Islet-like cluster · Glucose response

Received: September 8, 2008 / Accepted: March 1, 2009

H. Okura · Y. Fumimoto · Y. Sawa · T. Nishida
Department of Surgery, Osaka University Graduate School of Medicine, Osaka, Japan

H. Okura
Japan Society for the Promotion of Science, Tokyo, Japan

H. Komoda · A. Matsuyama (✉)
Laboratory for Somatic Stem Cell Therapy, Foundation of Biomedical Research and Innovation, TRI305, 1-5-4 Minatojima-minamimachi, Chuo-ku, Kobe 650-0047, Japan
Tel. +81-78-304-8706; Fax +81-78-304-8707
e-mail: akifumi-matsuyama@umin.ac.jp

C.-M. Lee · A. Matsuyama
Medical Center for Translational Research, Osaka University Hospital, Osaka, Japan

## Introduction

Type 1 diabetes mellitus results from the destruction of insulin-producing beta cells by autoimmune responses. Although modern insulin regimens are improving outcomes,[1] the successes achieved over the past few decades by transplantation of whole pancreas and isolated islets suggests that diabetes can be cured by replenishment of deficient beta cells. Transplantation therapy was established by Shapiro et al., and many patients received islet transplantation and a large population of recipients did not need further insulin therapy.[2,3] However, islets must be obtained from donors, but the resources are restricted and only a small proportion of patients can receive such transplantations. To overcome this problem, regenerative medicine for insulin-producing cells has been explored. Recently, it has been reported that insulin-producing cells could be differentiated from embryonic stem (ES) cells.[4–9] However, the sources of ES cells are limited; ES cell-derived insulin-producing cells are not available worldwide. The limited supply of such ES cells has led to the generation of insulin-producing cells from somatic stem cells. If we can generate insulin-producing cells from adult somatic stem cells, autologous insulin-producing cells might be used for diabetic patients and inappropriate human leukocyte antigen (HLA) matching could be avoided.

This investigation was initiated to establish a method for generating insulin-producing islet-like clusters from adipose tissue-derived stromal cells (ADSCs), since the adipose tissue resection technique is easy and safe. Our strategy was to transdifferentiate ADSCs into islet-like clusters through multiple steps. The generated islet-like clusters secreted insulin in response to glucose stimulation and nonglucose secretagogues, and expressed various molecules that resembled those expressed by pancreatic beta cells, such as Isl-1, Pax4, Pax6, pancreatic duodenal homeobox 1 (Pdx1), prohormone convertase (PC) 1/3, PC2, Kir6.2, glucose transporter (Glut) 2, glucokinase (GK), and insulin. Here we report that ADSCs can be transdifferentiated to form islet-like clusters that produce insulin. It is hoped that these

islet-like clusters can be used clinically in the near future for patients with type 1 diabetes mellitus.

## Materials and methods

### Adipose tissues from human subjects

Excess omental adipose tissues were resected from *the* gastro-omental artery during coronary artery bypass graft operation and excess subcutaneous adipose tissue *was resected* during mammary reconstruction procedures *in ten* subjects *[four* men and *six* women, 55 ± 5 years of age (mean ± SEM); range 40–60 *years]* who had given informed consent. The protocol was approved by the Review Board for Human Research of Osaka University Graduate School of Medicine. All subjects fasted *for* at least 10 h before surgery. None was taking steroids or thiazolidinediones. *A total of 1*–10 g of abdominal subcutaneous (external to the fascia superficialis) and greater omental adipose tissue *was* obtained from each subject.

### Isolation and culture of ADSCs

ADSCs were isolated as reported previously with minor modification.[10] In brief, adipose tissue was minced and then digested in Hank's balanced salt solution (HBSS) containing 0.075% collagenase (Sigma-Aldrich, St. Louis, MO, USA) in a shaking water bath *at 37°C* for 1 h. Digests were filtered with *a* cell strainer (BD Biosciences, San Jose, CA, USA) and centrifuged at 800 g for 10 min. Red blood cells were excluded using density gradient centrifugation with Lymphoprep (*density* = 1.077) (Nycomed, Oslo, Norway). The cells were then plated using Dulbecco's *modified* Eagle's *medium* (DMEM) with 10% defined *fetal bovine serum (FBS)*. After 24 h, the adherent cells were washed extensively, treated with ethtylenediaminetetraacetic acid (EDTA), and the suspended cells were replated at a density 10000 cells/cm$^2$ on human fibronectin-coated dishes in medium I: 60% DMEM low glucose, 40% MCDB201 (Sigma-Aldrich St. Louis, MO, USA), 10 µg/*ml* EGF (PeproTech, GmbH, Hamburg, Germany), 1 nM dexamethasone, 100 µM ascorbic acid, and 5% FBS. After three to five passages, the ADSCs were used in the experiments.

### In vitro differentiation procedure

The cells were treated with trypsin-EDTA to dissociate them, and single cells were obtained and then suspended in medium II [80% knockout-DMEM (Invitrogen, Carlsbad, CA, USA), 20% defined FBS, 1 mM glutamine, and 1% nonessential amino acid (both from Invitrogen)] and applied to low-attachment culture dishes (Hydrocell; CellSeed, Tokyo, Japan.). Within one day, cells were self-aggregated into spheroids, named adipospheres. The resultant adipospheres (stage II) were cultured for 7 days with a change of medium every 3 days.

Although adipospheres resembled embryoid bodies, we traced the methods established by Segev et al.,[9] in which insulin-producing cells were regenerated from embryoid bodies, to obtain insulin-producing cells from ADSCs. Seven-day-old adipospheres (which consisted, on average, of 1000 cells) were plated at a density of 300 adipospheres per well in six-well plastic culture plates and grown for another week in medium III: DMEM/F-12 1:1, 10 mg/l insulin, 6.7 mg/l transferrin, 5.5 mg/l selenium (ITS), and 1 mM glutamine (all from Invitrogen) with a supplement of 5 µg/ml human fibronectin (stage III). After 1 week in the ITS-fibronectin (ITSF) medium, the cells were dissociated and plated on 0.1% gelatin-coated plastic tissue-culture plates (BD Biosciences) at a concentration of 100000/ml in medium IV: DMEM/F-12 1:1 with N2 supplement, B27 (with vitamine A) media (both from Invitrogen), 1 mM glutamine, and 10 ng/ml basic fibroblast growth factor (bFGF, Invitrogen). These cells expanded throughout the week; the media was changed every other day.

In the next step (stage V), the cells were cultured in medium V: DMEM free of glucose/F-12 1:1, supplemented with N2 and B27 (without vitamine A) media, 1 mM glutamine, 10 mM nicotinamide, and 10 nM exendin-4 (both from Sigma-Aldrich). After 7 days of culture in medium V, the cells were dissociated and applied onto low-attachment culture dishes (Hydrocell) to grow in suspension with medium V (stage VI).

### Reverse transcription polymerase chain reaction

Total RNA was isolated from differentiated ADSCs using an RNAeasy kit (QIAGEN, Hilden, Germany). After treatment with DNase, cDNA was synthesized from 500 ng total RNA using Superscript III reverse transcriptase RNase H minus (Invitrogen). The absence of DNA contamination in RNA samples was confirmed by the polymerase chain reaction (PCR) primers flanking an intron. Primers and the reaction conditions are described in Table 1. The PCR products were fractionated by 2% agarose gel electrophoresis.

### Insulin secretion

The islet clusters obtained from the above procedure were rinsed three times in RPMI1640 (11879–020, Invitrogen) and preincubated for 1 h with the RPMI1640 containing 0.5% bovine serum albumin and 3.3 mM glucose. The masses of the clusters were expressed as islet equivalent (IEQ).[11] The clusters were then incubated for 2 h in RPMI1640 with 16.7 mM glucose and chased in RPMI1640 with 3.3 mM glucose with or without reagents such as theophylline (100 µM), isobutyl-methyl xanthine (IBMX) (100 µM), tolbutamide (10 µM), carbachol (100 µM), and nifedipine (50 µM) (all from Sigma-Aldrich). Then the conditioned media was analyzed for insulin and C-peptide levels. The insulin concentration was measured using an enzyme-linked immunosorbent assay (ELISA) kit (Merco-

**Table 1.** Primers and reaction conditions for the polymerase chain reaction

| Name | Sequence | Annealing (°C) | Size (bp) |
|---|---|---|---|
| Insulin | | | |
| F | AGGCTTCTTCTACACA | 65 | 245 |
| R | CAGGCTGCCTGCACCA | | |
| Glucagon | | | |
| F | AGGCAGACCCACTCAGTGA | 55 | 308 |
| R | AACAATGGCGACCTCTTCTG | | |
| Somatostatin | | | |
| F | TGCGCTGTCCATCGTCCT | 55 | 258 |
| R | GCCATAGCCGGGTTTGAGTT | | |
| IAPP | | | |
| F | GAGAGAGCCACTGAATTACTTGCC | 60 | 471 |
| R | CCTGACCTTATCGTGATCTGCC | | |
| Nestin | | | |
| F | AGAGGGGAATTCCTGGAG | 60 | 312 |
| R | CTGAGGACCAGGACTCTCTA | | |
| Is11 | | | |
| F | GATTTCCCTATGTGTTGGTTGC | 60 | 812 |
| R | CTTCCACTGGGTTAGCCTGTAA | | |
| Nkx6.1 | | | |
| F | GTTCCTCCTCCTCCTCTTCCTC | 60 | 381 |
| R | AAGATCTGCTGTCCGGAAAAAG | | |
| Pdx1 | | | |
| F | GGATGAAGTCTACCAAAGCTCACGC | 60 | 230 |
| R | CCAGATCTTGATGTGTCTCTCGGTC | | |
| Pax4 | | | |
| F | GTGGGCAGTATCCTGATTCAGT | 60 | 308 |
| R | TGTCACTCAGACACCTTTCTGG | | |
| Pax6 | | | |
| F | CCGAGAGTAGCGACTCCAG | 60 | 239 |
| R | CTTCCGGTCTGCCCGTTC | | |
| GLUT2 | | | |
| F | AGGACTTCTGTGGACCTTATGTG | 60 | 231 |
| R | GTTCATGTCAAAAAGCAGGG | | |
| Glucokinase | | | |
| F | AAGAAGGTGATGAGACGGATGC | 60 | 230 |
| R | CATCTGGTGTTTGGTCTTCACG | | |
| SUR1 | | | |
| F | GTGCACATCCACCACAGCACATGGCTTC | 62 | 429 |
| R | GTGTCTTGAAGAAGATGTATCTCCTCAC | | |
| KIR6.2 | | | |
| F | CGCTGGTGGACCTCAAGTGGC | 60 | 497 |
| R | CCTCGGGGCTGGTGGTCTTGCG | | |
| PC1/3 | | | |
| F | TTGGCTGAAAGAGAACGGGATACATCT | 60 | 457 |
| R | ACTTCTTTGGTGATTGCTTTGGCGGTG | | |
| PC2 | | | |
| F | GCATCAAGCACAGACCTACACTCG | 60 | 309 |
| R | GAGACACAACCACCCTTCATCCTTC | | |
| E-cadherin | | | |
| F | AGAACAGCACGTACACAGCC | 60 | 530 |
| R | CCTCCGAAGAAACAGCAAGA | | |
| GAPDH | | | |
| F | GTCAGTGGTGGACCTGACCT | 60 | 394 |
| R | AGGGGAGATTCAGTGTGGTG | | |

The number of cycles was 35 in each case
Pax, Paired box gene

dia, Uppsala, Sweden), which detects human insulin with no cross-reactivity to proinsulin or C-peptide. C-peptide levels were also measured by an ELISA kit (Mercodia).

## Immunohistochemistry

Stage VI clusters were fixed for 24 h in 4% paraformaldehyde in phosphate-buffered saline (PBS), permeabilized using 0.5% Triton X-100 in PBS, and then incubated overnight with the primary antibody guinea-pig anti-insulin (1:100, Dako, Glostrup, Denmark) with either rabbit anti-C-peptide (1:100, Linco, St. Charles, MO, USA), rabbit anti-glucagon (1:100, Dako), or rabbit anti-somatostatin (1:200, Dako). After rinsing, secondary antibodies were added to the samples, which were then incubated for another 1 h at room temperature. Finally, the cells were rinsed three times, sliced into 10-µm slices, and mounted

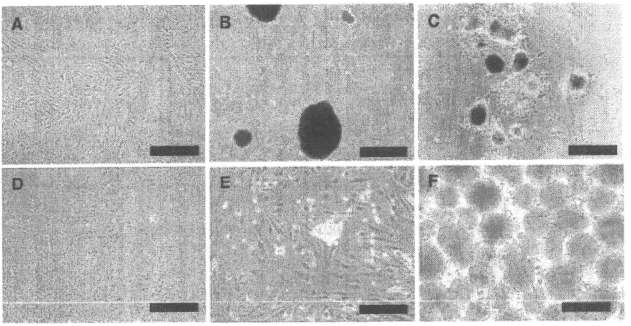


**Fig. 1A–F.** General outline of the differentiation protocol, which consists of six stages. **A** Stage I: growth of adipose tissue-derived stromal cells (*bar* 500 µm). **B** Stage II: formation of adipospheres in suspension (*bar* 500 µm). **C** Stage III: plating adipospheres in medium I for 1 week (*bar* 500 µm). **D** Stage IV: dissociating the cells and plating them in medium II on gelatin-coated dishes for 1 week (*bar* 500 µm). **E** Stage V: change to medium III and culture for 1 week (*bar* 250 µm). **F** Stage VI: dissociation of the cells and growing them in suspension in low-attachment dishes with medium III for 3 days to form clusters (*bar* 250 µm)

with Permaflur (Thermo Fisher Scientific, Waltham, MA, USA). The slides were examined using a fluorescence microscope (Floview FV1000, Olympus, Tokyo, Japan).

## Results

### Multistep procedure for differentiation of ADSCs into insulin-producing islet-like clusters

To promote the differentiation of human ADSCs into insulin-producing cells, we applied the procedure outlined in Fig. 1. In the first stage, ADSCs were expanded and passaged three to five times. In the next stage, ADSCs were cultured in suspension. Within 48 h of incubation, these cells started forming cell aggregates, named adipospheres, which grew bigger with time, forming spheroids. In the third stage, the adipospheres were plated and expanded in insulin-transferrin-selenium-fibronectin (ITSF) medium. In the fourth stage, the expanded cells in stage III were collected individually and cultured in N2 and B27 supplemented with basic fibroblast growth factor (bFGF). The fourth stage cells could be split and passaged. In the fifth stage, these cells were cultured in a medium lacking bFGF and vitamin A, and containing nicotinamide and exendin-4. In the last stage (stage VI), the cells obtained in stage V were cultured in suspension. Within 3 days of incubation, the cells started forming cell islet-like aggregates.

### Dynamics of pancreatic gene expression during differentiation of ADSCs into insulin-producing clusters

Analysis with reverse transcription polymerase chain reaction (RT-PCR) demonstrated enhanced expression of pancreatic genes in the differentiated insulin-producing islet-like clusters of ADSCs (Fig. 2). Insulin was expressed in stage VI, while other pancreatic hormones, such as glucagon, somatostatin and islet amyloid polypeptide (IAPP), were observed in stages V and VI. Nestin appeared in stage II

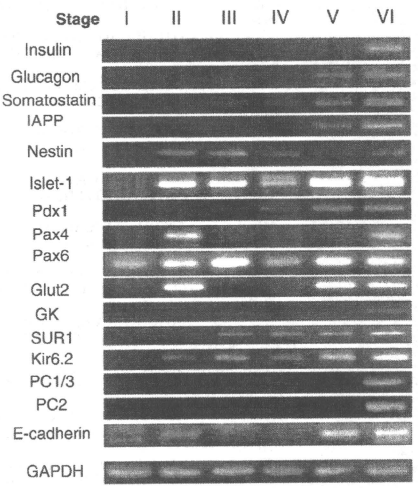


**Fig. 2.** Reverse transcription polymerase chain reaction (RT-PCR) analysis of pancreatic gene expression at the six differentiation stages. Total RNA isolated from the cells of each differentiation step was subjected to RT-PCR analysis with primers for the indicated genes. *IAPP*, islet amyloid polypeptide; *Pdx1*, pancreatic duodenal homeobox 1; *Glut2*, glucose transporter 2; *GK*, glucokinase; *PC*, prohormone convertase; *GAPDH*, Glyceraldehyde 3 phosphate dehydrogenase

and was highly expressed in stages II, III, and VI. Further examination of the transcriptional factors related with beta cell development showed expression of islet-1 in all stages except stage I, and expression of Pdx1 in stage IV with further increase with differentiation. Expression of Pax4 appeared in stages II and VI, and that of Pax6 was noted in all stages of differentiation. Next, we examined messages of *Glut2*, *GK*, the $K_{ATP}$-channel genes *Kir6.2* and *SUR1*, *PC1/3*, and *PC2*. *Glut2* appeared in stage II, disappeared, and then reappeared in stages V and VI. *GK* was detected in stage III and the final stage. *Kir6.2* was expressed in stages II to VI, and *SUR1* was expressed in stages III to VI. *PC1/3* and *PC2* were observed in stage VI. Thus, the generated insulin-producing clusters could process proinsulin into insulin and generate C-peptide. *E-cadherin* was observed in stages V and VI, and enhanced pancreatic beta cell cluster formation into islets. These results indicate that the adipocyte-derived differentiated cells can transcribe, process, and secrete insulin in response to glucose.

### Islet-like clusters release insulin in a similar way topancreatic islets

The generated clusters were examined for their insulin-secretion potential (Fig. 3A). The glucose challenge tests showed that the generated clusters secreted insulin in the conditioned media at concentrations of 50.9 ± 1.9 μU/1000 IEQ (islet equivalents) (mean ± SEM) at high glucose challenge (16.7 mM) and 26.1 ± 1.3 μU/1000 IEQ at low glucose challenge (3.3 mM) (Fig. 3A). Next, we examined the effects of 10 μM IBMX on glucose insulin response and C-peptide secretion. IBMX increased insulin release from adipocyte-derived differentiated cells 3.6-fold to 185.0 ± 17.0 μU/1000 IEQ and C-peptide release increased 2.8-fold from 1.6 ± 0.1 to 4.4 ± 0.5 ng/1000 IEQ (Fig. 3A). To determine whether these cells regulate insulin release via physiological signaling pathways, we examined the effects of several agonists and antagonists on insulin secretion (Fig. 3B). In the presence of high glucose levels, theophylline (100 μM) induced a 3.6-fold increase in insulin secretion; tolbutamide (10 μM), an inhibitor of the $K_{ATP}$-channel, a 4.2-fold increase; and carbachol (100 μM), an agonist of muscarinic cholinergic receptors, a 1.6-fold increase. Nifedipine (50 μM), a blocker of $Ca^{2+}$ channels present in beta cells, did not alter insulin secretion in response to low (25.7 ± 0.6 μU/1000 IEQ) or high glucose levels (29.3 ± 0.6 μU/1000 IEQ). These results indicate that glucose induced the pancreatic machinery in the differentiated cells to release insulin.

### Generated islet-like clusters express insulin, glucagon, somatostatin, and C-peptide in a similar way to pancreatic islets

Stage VI clusters were subjected to immunofluorescence analysis for the expression of insulin, C-peptide, glucagon, and somatostatin (Fig. 4). Insulin-positive cells were the major population of cells among the generated islet-like

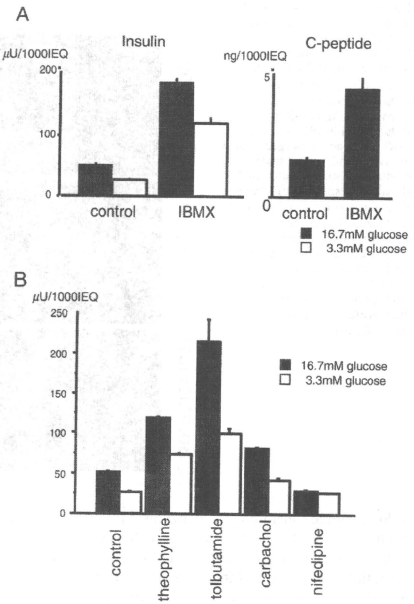


**Fig. 3A,B.** Regenerated insulin-producing cluster derived from adipose tissue-derived stromal cells. **A** Glucose-induced insulin and C-peptide release in response to low (3.3 mM) and high (16.7 mM) glucose levels. **B** Effects of various agonists and antagonists on insulin secretion. Data represent the effects of theophylline, isobutyl-methyl xanthine (*IBMX*), tolbutamide, carbachol, and nifedipine. All data represent the mean ± SEM of experiments performed in triplicate

clusters. As shown in Fig. 4F, insulin was localized inside the cells (arrowheads) while glucagon was identified on the cell surface (arrows). Only a small number of cells expressed somatostatin (Fig. 4G; arrowhead). These expression patterns of pancreatic hormones in the generated clusters were similar to those identified in pancreatic islets.[10] Almost all insulin-expressing cells coexpressed C-peptide, indicating the production of insulin (Fig. 4C). A substantial number of cells coexpressed insulin and glucagon (Fig. 4F), and insulin and somatostatin (Fig. 4I), in the same way as immature pancreatic endocrine cells described in the development of the pancreas.[10] These results indicate that the generated islet-like clusters derived from ADSCs resemble pancreatic islets.

## Discussion

Recent studies have demonstrated the feasibility of generating insulin-producing cells from progenitor cells of various

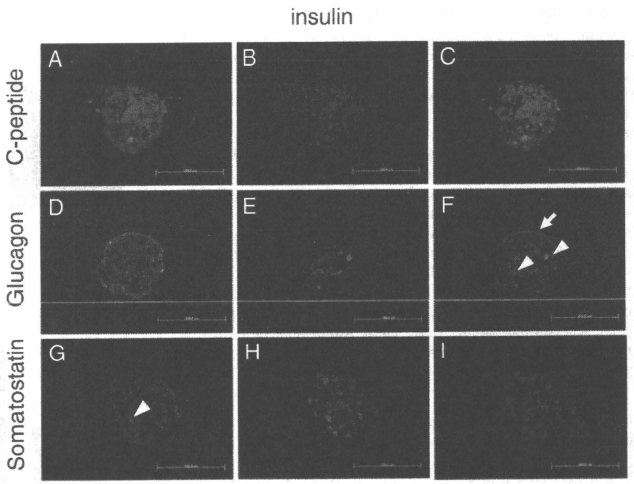


**Fig. 4.** Immunocytochemical analysis of stage VI clusters. Immunohistochemical analysis for insulin, C-peptide, somatostatin, and glucagon. **A** C-peptide staining, **D** somatostatin staining, **G** glucagon staining (all in *green*), **B**, **E**, and **H** insulin staining (*red*). **C**, **F**, and **I** merged images of insulin and second marker (C-peptide, somatostatin, and glucagon, respectively) (*orange*). **F** Insulin was localized inside the cells (*arrowheads*), while glucagon was identified on the cell surface (*arrow*). **G** Only a small number of cells expressed somatostatin (*arrowhead*). Photographs taken using a fluorescence microscope (*bar* 100 µm)

cellular sources, including the pancreas,[12] liver,[13,14] intestinal epithelium,[15] and bone marrow,[16] as well as pluripotent ES cells from mice and humans.[4–9] Despite their promising potential, it may prove difficult to obtain a sufficient quantity of autologous adult stem cells from these sources. To overcome these limitations, we explored the possibility of using human adipose tissues as a source for transdifferentiation into insulin-producing cells. Adipose tissue is a safe and abundant source of large amounts of somatic stem cells. In the present study, we generated functional insulin-producing cells from human ADSCs using a multistep in vitro differentiation procedure. These studies provide direct evidence that human ADSCs could be programmed in vitro to become functional insulin-producing cells.

To differentiate human ADSCs into insulin-producing cells, we used a six-step transdifferentiation procedure. To design the protocol, we supposed that noncommitted cells were expanded in the first step, multipotent cells were selected in the second step, endodermal-committed cells were selected in the third step, the committed cells were expanded in the fourth step, these cells were committed into pancreatic cells in the fifth step, and in the sixth step these cells were expected to mature into insulin-producing cells.

In detail, in the first step, human ADSCs were grown to expand their numbers and their undifferentiated properties were maintained with selenium. Selenium is used in serum-free cultivation to protect mesenchymal stem cells against damage due to cultivation and to maintain their properties as stem cells.[17] The second step was performed to select and enrich the undifferentiated cells. By using floating culture in stage II, undifferentiated cells formed spheroids, named adipospheres. Adipospheres expressed islet-1, nestin, and Pax4, as shown in Fig. 2. Previous studies indicated that cells positive for islet-1, nestin, and/or Pax4 are pancreatic endocrine progenitor cells.[18–20] Mesenchymal stem cells were grown under floating conditions where they generated spheroids. Multipotent stem cells in the form of spheroids are also known as neurospheres, and have been described as differentiating into neuronal lineages.[20] In the third step, we were able to expand the nestin-positive cells and increase their numbers under insulin-transferrin-selenite-fibronectin (ITSF) serum-free conditions. Because of the similarities between the development of beta cells and that of neuroepithelial cells,[21] a similar transient expression of nestin was reported to occur in human insulin-producing beta cell precursors.[18,19] In the fourth step, the cells were transferred to a medium containing N2, B27, and bFGF. N2 and B27 were first designated as supplements for serum-free media for culture of neural cells primarily for protection against oxidants. Just as for neural cells, beta cells are sensitive to reactive oxygen species.[22] bFGF and vitamin A have growth promoting effects on pancreatic epithelial cells reported as precursors of beta cells.[6,23–25] At the end of the differentiation procedure, bFGF and vitamin A were withdrawn and nicotinamide and exendin-4 were added to promote maturation of precursor cells into insulin-producing cells. Nicotinamide increases the rate of proinsulin biosynthesis, and the resultant increase in insulin production and content is due to formation of new beta cells through differentiation.[26,27] Exendin-4 has been reported to stimulate both the differentiation of beta cells from ductal progenitor cells and proliferation of beta cells when given to rats.[28,29] In the final step, the cells were cultivated under floating conditions to enhance the maturation of progenitor cells into beta cells.[6,30] Taken together, almost all the steps of the procedure seem

to promote the transdifferentiation of human ADSCs into insulin-producing clusters.

Recent studies illustrated that when cultured in vitro, bone marrow-derived mesenchymal stem cells obtained from mice and rats could be differentiated into insulin-producing cells.[31,32] In addition, Sun et al. demonstrated that human bone marrow-derived stem cells can differentiate into insulin-producing cells under appropriate conditions in vitro.[33] In the differentiating conditions, the bone marrow-derived mesenchymal stem cells were cultured with bFGF, betacellulin, activin A, and nicotinamide under high glucose conditions. In our procedures, ADSCs were cultured with bFGF, exendin-4, and nicotinamide under low glucose conditions. Timper et al. supposed that ADSCs could express insulin message after 3 days of cultivation and differentiate into pancreatic beta cells.[34] Unfortunately, they could not show that the insulin-producing cells processed according to their method could secrete insulin in response to glucose challenge, supposing that their cells did not fully differentiate into pancreatic beta cells but into their precursors or progenitors. In our method, the cells were cultured under floating conditions in the final step in differentiation. To fully differentiate into insulin-producing cells, cell-cluster formation might be critical, as suggested by Segev et al.[9]

In the clinical context, our present study demonstrated the potential for cell-based therapy of diabetes involving the generation of autologous insulin-producing cells in vitro from ADSCs. Although autoimmunity against autologous regenerated islets could be a concern, these in vitro-generated insulin-producing cells could, in theory, provide a potentially unlimited source of islet-like cells without the limitation of immune rejection based on alloimmunity. However, because there are multifactorial influences in the transdifferentiation of ADSCs into competent insulin-producing cells, there are many questions left unanswered, and unresolved issues remain. In addition, the insulin-producing capacity of the ADSC-derived islet-like clusters was similar to that of ES cell-derived islet-like clusters but was less than that of isolated islets by a factor 10 to 100.[9,11] Obviously, further research is required to address these important questions, yet we believe the results demonstrated in this study provide direct evidence supporting the notion that transdifferentiation of ADSCs to insulin-producing cells may represent a viable therapeutic option for type 1 diabetes.

**Acknowledgments** This study was supported in part by a Grant-in-Aid for Akifumi Matsuyama from Kobe Translational Research Cluster, the Knowledge Cluster Initiative, the Ministry of Education, Culture, Sports, Science and Technology of Japan (MEXT), and in part by a Grant-in-Aid for Yoshiki Sawa from the New Energy and Industrial Technology Development Organization (NEDO), Japan.

## References

1. Epidemiology of Diabetes Interventions and Complications Research Group. Sustained effect of intensive treatment of type 1 diabetes mellitus on development and progression of diabetic nephropathy: the Epidemiology of Diabetes Interventions and Complications (EDIC) study. JAMA 2003;290:2159–2167
2. Shapiro AM, Lakey JR, Ryan EA, Korbutt GS, Toth E, Warnock GL, Kneteman NM, Rajotte RV. Islet transplantation in seven patients with type 1 diabetes mellitus using a glucocorticoid-free immunosuppressive regimen. N Engl J Med 2000;343:230–238
3. Robertson RP. Islet transplantation as a treatment for diabetes – a work in progress. N Engl J Med 2004;350:694–705
4. Soria B, Roche E, Berna G, León-Quinto T, Reig JA, Martin F. Insulin-secreting cells derived from embryonic stem cells normalize glycemia in streptozotocin-induced diabetic mice. Diabetes 2000;49:157–162
5. Assady S, Maor G, Amit M, Itskovitz-Eldor J, Skorecki KL, Tzukerman M. Insulin production by human embryonic stem cells. Diabetes 2001;50:1691–1697
6. Lumelsky N, Blondel O, Laeng P, Velasco I, Ravin R, McKay R. Differentiation of embryonic stem cells to insulin-secreting structures similar to pancreatic islets. Science 2001;292:1389–1393
7. Kahan BW, Jacobson LM, Hullett DA, Ochoada JM, Oberley TD, Lang KM, Odorico JS. Pancreatic precursors and differentiated islet cell types from murine embryonic stem cells: an in vitro model to study islet differentiation. Diabetes 2003;52:2016–2024
8. Leon-Quinto T, Jones J, Skoudy A, Burcin M, Soria B. In vitro directed differentiation of mouse embryonic stem cells into insulin-producing cells. Diabetologia 2004;47:1442–1451
9. Segev H, Fishman B, Ziskind A, Shulman M, Itskovitz-Eldor J. Differentiation of human embryonic stem cells into insulin-producing clusters. Stem Cells 2004;22:265–274
10. Djian P, Roncari DAK, Hollenberg CH. Influence of anatomic site and age on the replication and differentiation of rat adipocyte precursors in culture. J Clin Invest 1983;72:1200–1208
11. Komoda H, Miyagawa S, Omori T, Takahagi Y, Murakami H, Shigehisa T, Ito T, Matsuda H, Shirakura R. Survival of adult islet grafts from transgenic pigs with *N*-acetylglucosaminyltransferase-III (GnT-III) in cynomolgus monkeys. Xenotransplantation 2005;12:209–216
12. Seaberg RM, Smukler SR, Kieffer TJ, Enikolopov G, Asghar Z, Wheeler MB, Korbutt G, van der Kooy D. Clonal identification of multipotent precursors from adult mouse pancreas that generate neural and pancreatic lineages. Nat Biotechnol 2004;22:1115–1124
13. Zalzman M, Gupta S, Giri RK, Berkovich I, Sappal BS, Karnieli O, Zern MA, Fleischer N, Efrat S. Reversal of hyperglycemia in mice by using human expandable insulin-producing cells differentiated from fetal liver progenitor cells. Proc Natl Acad Sci USA 2003;100:7253–7258
14. Yang L, Li S, Hatch H, Ahrens K, Comelius JG, Petersen BE, Peck AB. In vitro trans-differentiation of adult hepatic stem cells into pancreatic endocrine hormone-producing cells. Proc Natl Acad Sci USA 2002;99:8078–8083
15. Yoshida S, Kajimoto Y, Yasuda T, Watada H, Fujitani Y, Kosaka H, Gotow T, Miyatsuka T, Umayahara Y, Yamasaki Y, Hori M. PDX-1 induces differentiation of intestinal epithelioid IEC-6 into insulin-producing cells. Diabetes 2002;51:2505–2513
16. Ianus A, Holz GG, Theise ND, Hussain MA. In vivo derivation of glucose-competent pancreatic endocrine cells from bone marrow without evidence of cell fusion. J Clin Invest 2003;111:843–850
17. Ebert R, Ulmer M, Zeck S, Meissner-Weigl J, Schneide D, Stopper H, Schpp N, Kassem M, Jacob F. Selenium supplementation restores the antioxidative capacity and prevents cell damage in bone marrow stromal cells in vitro. Stem Cells 2006;24:1226–1235
18. Zulewski H, Abraham EJ, Gerlach MJ, Daniel PB, Moritz W, Müller B, Vallejo M, Thomas MK, Habener JF. Multipotential nestin-positive stem cells isolated from adult pancreatic islets differentiate ex vivo into pancreatic endocrine, exocrine, and hepatic phenotypes. Diabetes 2001;50:521–533
19. Blyszczuk P, Czyz J, Kania G, Wagner M, Roll U, St-Onge L, Wobus AM. Expression of Pax4 in embryonic stem cells promotes differentiation of nestin-positive progenitor and insulin-producing cells. Proc Natl Acad Sci USA 2003;100:998–1003
20. Eberhardt M, Salmon P, von Mach MA, Hengstler JG, Brulport M, Linscheid P, Seboek D, Oberholzer J, Barbero A, Martin I, Müller B, Trono D, Zulewski H. Multipotential nestin and Isl-1

positive mesenchymal stem cells isolated from human pancreatic islets. Biochem Biophys Res Commun 2006;345:1167–1176
21. Kang SK, Putnam LA, Ylostalo J, Popescu IR, Dufour J, Belousov A, Bunnell BA. Neurogenesis of Rhesus adipose stromal cells. J Cell Sci 2004;17:289–299
22. Evans JL, Goldfine ID, Maddux BA, Grodsky GM. Are oxidative stress-activated signaling pathways mediators of insulin resistance and beta-cell dysfunction? Diabetes 2003;52:1–8
23. Schuldiner M, Yanuka O, Itskovitz-Eldor J, Melton DA, Benvenisty N. From the cover: effects of eight growth factors on the differentiation of cells derived from human embryonic stem cells. Proc Natl Acad Sci USA 2000;97:11307–11312
24. Soria B. In vitro differentiation of pancreatic beta-cells. Differentiation 2001;68:205–219
25. Ogneva V, Martinova Y. The effect of in vitro fibroblast growth factors on cell proliferation in pancreas from normal and streptozotocin-treated rats. Diabetes Res Clin Pract 2002;57: 11–16
26. Otonkoski T, Beattie GM, Mally MI, Ricordi C, Hayek A. Nicotinamide is a potent inducer of endocrine differentiation in cultured human fetal pancreatic cells. J Clin Invest 1993;92: 1459–1466
27. Vaca P, Berna G, Martin F, Soria B. Nicotinamide induces both proliferation and differentiation of embryonic stem cells into insulin-producing cells. Transplant Proc 2003;5:2021–2023
28. Xu G, Stoffers DA, Habner JF, Bonner-Weir S. Exendin-4 stimulates both beta-cell replication and neogenesis, resulting in increased beta-cell mass and improved glucose tolerance in diabetic rats. Diabetes 1999;48:2270–2276
29. Abraham EJ, Leech CA, Lin JC, Zulewski H, Habener JF. Insulinotropic hormone glucagon-like peptide-1 differentiation of human pancreatic islet-derived progenitor cells into insulin-producing cells. Endocrinology 2002;143:3152–3161
30. Itkin-Ansari P, Demeterco C, Bossie S, de la Tour DD, Beattie GM, Movassat J, Mally MI, Hayek A, Levine F. PDX-1 and cell–cell contact act in synergy to promote delta-cell development in a human pancreatic endocrine precursor cell line. Mol Endocrinol 2000;14:814–822
31. Tang DQ, Cao LZ, Burkhardt BR, Xia CQ, Litherland SA, Atkinson MA, Yang LJ. In vivo and in vitro characterization of insulin-producing cells obtained from murine bone marrow. Diabetes 2004;53:1721–1732
32. Oh SH, Muzzonigro TM, Bae SH, LaPlante JM, Hatch HM, Petersen BE. Adult bone marrow-derived cells trans-differentiating into insulin-producing cells for the treatment of type I diabetes. Lab Invest 2004;84:607–617
33. Sun Y, Chen L, Hou XG, Hou WK, Dong JJ, Sun L, Tang KX, Wang B, Song J, Li H, Wang KX. Differentiation of bone marrow-derived mesenchymal stem cells from diabetic patients into insulin-producing cells in vitro. Clin Med J 2007;120:771–776
34. Timper K, Seboek D, Eberhardt M, Linscheid P, Christ-Crain M, Keller U, Müller B, Zulewski H. Human adipose tissue-derived mesenchymal stem cells differentiate into insulin-, somatostatin-, and glucagon-expressing cells. Biochem Biophys Res Commun 2006;341:1135–1140

TISSUE ENGINEERING: Part C
Volume 15, Number 00, 2009

DOI: 10.1089/ten.tec.2008.0555

TEN-2008-0555-Fumimoto
Type: other

# Creation of a Rich Subcutaneous Vascular Network with Implanted Adipose Tissue–Derived Stromal Cells and Adipose Tissue Enhances Subcutaneous Grafting of Islets in Diabetic Mice

AU1 ▶ Yuichi Fumimoto, M.D.,[1] Akifumi Matsuyama, M.D., Ph.D.,[2,3] Hiroshi Komoda, M.D., Ph.D.,[3] Hanayuki Okura, M.S.,[1,2] Chun Man Lee, M.D., Ph.D.,[2] Anna Nagao,[2] Toshirou Nishida, M.D., Ph.D.,[1] Toshinori Ito, M.D., Ph.D.,[4] and Yoshiki Sawa, M.D., Ph.D.[1,2]

Subcutaneous tissue was proposed as an optimal transplant site for islets in treatment for type I diabetes mellitus. However, vascular networks in subcutaneous tissue are too poor in their natural state to allow survive and function of the transplanted graft. This study examined whether subcutaneous implantation of adipose tissue–derived stromal cells (ADSCs) combined with minced adipose tissue could form vascular-rich beds suitable to support islet transplantation. ADSCs were isolated from male C57BL/6J mouse inguinal subcutaneous adipose tissue. ADSCs and minced adipose tissue were implanted syngeneically in subcutaneous tissue of the back of recipient mice. Four weeks later, vascularization in the implanted subcutaneous tissue was evaluated, and islets were transplanted onto the vascularized pockets. Mice that received ADSCs mixed with minced adipose tissue showed a richly vascularized pocket of tissue with significantly higher capillary density than in mice implanted with either ADSCs or minced adipose tissue only. All recipient mice of the combination ADSCs and minced adipose tissue group showed correction in blood glucose level within a week after islet transplantation and maintained normoglycemia for over 8 weeks. These mice became hyperglycemic again after removal of the subcutaneous grafts. This novel method will expand the indications for islet transplant therapy and potential clinical application of cell-based therapy.

## Introduction

CLINICAL ISLET TRANSPLANTATION is widely used as a surgical treatment for type I diabetes mellitus with isolated islets commonly injected into the liver through the portal vein.[1] Although now relatively safe, this procedure is still associated with complications such as bleeding and high portal pressure,[2] and repeated injections of islets to normalize blood sugar levels may increase the incidence of these complications.[2] In addition, the immediate blood-mediated inflammatory reaction following injection into the liver could damage the grafted islets.[3,4] Thus, alternative transplant sites should be investigated to reduce these adverse events. Previous studies have explored the subcapsular kidney space, spleen, intramuscular tissue, and omental pouch as potential transplant sites.[5–8] However, the invasive nature of accessing these sites, among other reasons, reduces their value for clinical transplantation.

Subcutaneous tissue has many advantages as a transplant site for islets. The area is accessible with minimal invasiveness under local anesthesia, it provides massive transplantable capacity, and the tissue is removable if severe adverse events eventuate due to the transplanted grafts. However, vascular networks in subcutaneous tissue are too poor to maintain insulin-producing function.[9] Some studies described functional grafted islets with insulin-producing function in subcutaneous tissue pretreated with angiogenic factors and synthetic vascularizing devices to form vascular-rich

[1]Department of Surgery (E1), Osaka University Graduate School of Medicine, Suita, Japan.
[2]Medical Center for Translational Research, Osaka University Hospital, Suita, Japan.
[3]Laboratory for Somatic Stem Cell Therapy, Foundation of Biomedical Research and Innovation, Kobe, Japan.
[4]Complementary and Alternative Medicine, Osaka University Graduate School of Medicine, Suita, Japan.

beds.[10–13] Unfortunately, these combined devices are difficult to apply clinically because the synthetic materials would need to remain in the body for a long term.

Adipose tissue–derived stromal cells (ADSCs) are multipotent progenitor cells capable of differentiating into endothelial cells.[14,15] In animal experiments, ADSCs induced postnatal neovascularization resulting in collateral formation, and improved the reperfusion of blood flow in femoral artery-ligated ischemic limb.[16,17] Further, ADSCs were used successfully to support and augment soft tissues after lipotransfer by vascularizing the transferred adipose tissue.[18] These reports indicated that transplantation of a mixture of ADSCs and minced adipose tissue could potentially form vascular-rich beds in subcutaneous tissue. This study further examines whether such a mixture could be implanted subcutaneously to vascularize pockets of tissue and support grafted islets for long-term function.

## Materials and Methods

### *Animals*

The study was conducted in C57BL/6J male mice (CLEA Japan, Inc., Tokyo, Japan) anesthetized with an intraperitoneal injection of 2.5% tribromoethanol. All transplant experiments were performed syngeneically. The Osaka University Graduate School of Medicine Standing Committee on Animals approved all experimental protocols.

### *Isolation of mouse ADSCs*

ADSCs were isolated from the inguinal subcutaneous adipose tissue of 8-week-old C57BL/6J male mice, as reported previously.[19] The cells were cultured in Stem Cell Medium (Nacalai Tesque, Kyoto, Japan) containing 10 ng/mL epidermal growth factor (EGF; PeproTech EC, London, UK), 1 nM dexamethasone, 100 μM ascorbic acid (both from Sigma–Aldrich Japan, Tokyo, Japan), and 5% fetal bovine serum (FBS; Invitrogen, Carlsbad, CA). The ADSCs were used for experiments after 3–5 passages.

### *Flow cytometric analysis*

The ADSCs were characterized by flow cytometry using fluorescein isothiocyanate (FITC)–conjugated mouse monoclonal antibodies to mouse Ly-6A/E (Sca-I), CD31, CD44, CD45, CD117 (all from BD Pharmingen, Franklin Lakes, NJ), and CD34 (Santa Cruz Biotechnology, Santa Cruz, CA). Isotype-identical antibodies served as controls. Analyses were performed using a FACSCalibur flow cytometer and CellQuest Pro software (BD Biosciences, Franklin Lakes, NJ).

### *Subcutaneous vascularization with ADSC and adipose tissue*

Eight-week-old C57BL/6J male mice were used as recipients. Recipient mice were divided into four groups, and implanted as follows to create a rich vascular network in the subcutaneous tissue: group I ($n=6$), ADSCs ($5\times10^5$ cells) mixed with minced inguinal adipose tissue (150 μL); group II ($n=5$), ADSCs ($5\times10^5$ cells) only; group III ($n=6$), minced inguinal adipose tissue (150 μL) only; and group IV ($n=6$), nothing implanted. To facilitate the islet transplant technique, a spacer made of nonbiodegradable and non-cell-adherent material (polyester, 10×12 mm) was subcutaneously implanted with each of the grafts. Specifically, a small incision was made at the back of recipient mice, and the subcutaneous tissue was split gently. A spacer was inserted in the split space in the subcutaneous tissue. Then, the graft of groups I and III mentioned above was implanted around a spacer. In group II, ADSCs with 300 μL phosphate buffered saline were injected into the subcutaneous tissue contacted with a spacer. In group IV, nothing is implanted except a spacer in the subcutaneous tissue. Finally, the incision was closed with 5-0 absorbable suture. Four weeks later, vascularization in the subcutaneous tissue was examined after removal of the spacer. Twelve-week-old C57BL/6J male mice that were not pretreated with ADSCs, adipose tissue, and a spacer were evaluated additionally as control mice ($n=5$).

### *Isolation of mouse islets*

Islets were isolated from 10-week-old C57BL/6J male mice as reported previously.[20] Briefly, type XI collagenase solution (0.5 mg/mL; Sigma-Aldrich Japan) was injected into the common bile duct of mice and digested for 25 min at 37°C. The digested fragments were collected and washed with Hanks' balanced salt solution (HBSS). Islets were purified through a discontinuous Ficoll gradient (Nacalai Tesque), and the islet-rich layer was collected for transplantation.

### *Subcutaneous islet transplantation*

Separate recipient mice of above four groups were set up for subcutaneous islet transplantation. Islet transplantation was performed 4 weeks after each pretreatments for vascularization. Recipient mice were made diabetic by a single peritoneal injection of streptozotocin (250 mg/kg body weight; Sigma-Aldrich Japan) at 7 days before islet transplantation. The diabetic mice were defined as having nonfasting blood glucose levels >350 mg/dL. Islets were transplanted into the subcutaneous tissue pockets of each group after removal of the spacer. All groups received 600 islets (group I, $n=7$; group II, $n=7$; group III, $n=5$; group IV, $n=5$). Blood glucose levels were measured once a week by tail snipping, using a portable glucose meter (Nipro Care Fast Meter; Nipro, Tokyo, Japan). After 8 weeks, the graft-bearing subcutaneous tissues from the recipient mice were evaluated by histological examination.

### *Intraperitoneal glucose tolerance test*

After overnight fasting, mice were injected intraperitoneally with glucose at 2 g/kg body weight. Blood glucose levels were measured at 0, 15, 30, 60, 90, and 120 min after glucose injection. Glucose tolerance was tested in recipient mice of group I ($n=5$) at 3 weeks after islet transplantation and in nondiabetic mice ($n=5$).

### *Histological and immunohistochemical examination*

Graft-bearing subcutaneous tissues were removed and processed for sectioning (4 μm thickness) and staining with hematoxylin and eosin. To evaluate vascularization and the function of the grafted islets, the graft specimens were also immunostained using an anti–von Willebrand factor (vWF) polyclonal antibody (1:1000; Chemicon-Millipore

Corporation, Billerica, MA) or anti-insulin polyclonal antibody (1:500; Santa Cruz Biotechnology), respectively. Vessels were identified by positive staining for von Willebrand factor and by morphology. Vessel number was evaluated by randomly counting the vessels in 10 different subcutaneous areas.

*Statistical analysis*

The pathologist who conducted the blood vessel counting was blinded to the method used in surgical preparation of the animal. Values are expressed as mean ± SD. Statistical comparisons among groups were performed with ANOVA

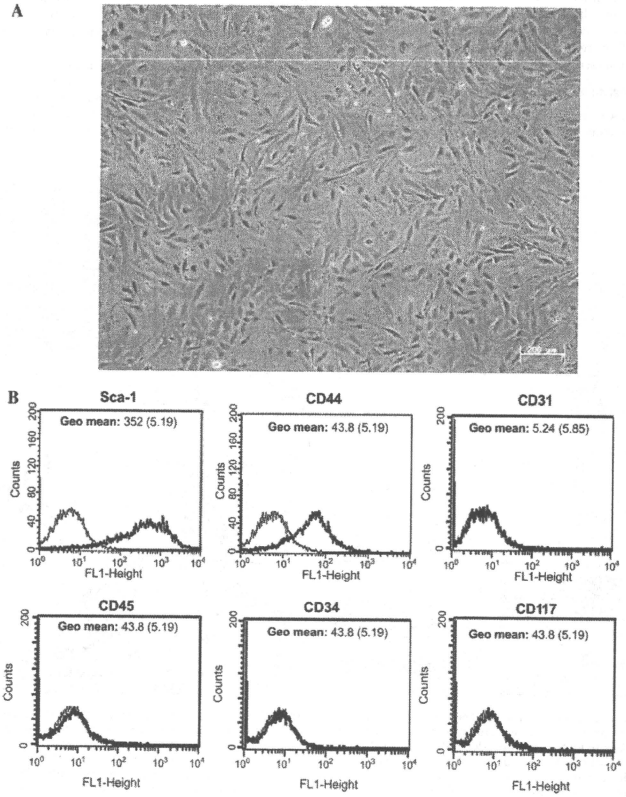


FIG. 1. Characteristics of isolated ADSCs. (A) A phase-contrast micrograph of cultured ADSCs isolated from mouse adipose tissue and cultured for four passages showing spindle-shaped morphology. (B) Flow cytometric analysis of expression of surface antigens on ADSCs using mouse monoclonal antibodies. All panels include an isotype-matched negative control (thin lines). As indicated, the antigens tested were Ly-6A/E (Sca-1), CD31, CD34, CD44, CD45, and CD117 (bold line).

for multiple comparisons. A $p$-value $<0.05$ was considered statistically significant.

## Results

### *Characterization of ADSCs*

The isolated ADSCs obtained from mouse inguinal adipose tissue were spindle-shaped in morphology (Fig. 1A). Flow cytometric analysis showed these cells to be positive for Ly-6A/E (Sca-I) and CD44 as surface markers of mesenchymal stem cells, but negative for CD31, CD34, CD45, and CD117 as hematopoietic and endothelial lineage markers (Fig. 1B). These results indicated that the ADSCs used in this study were mesenchymal stem cells.

### *Pocket creation for subcutaneous transplantation*

The ADSCs and minced adipose tissue were implanted together or alone in the subcutaneous tissue of the back in each group of mice, as detailed in the Materials and Methods section. In addition, a polyester spacer (Fig. 2A) was subcutaneously implanted with all grafts to facilitate the islet transplant technique. Four weeks later, the spacer was removed, leaving a subcutaneous tissue pocket into which islets could be easily transplanted (Fig. 2B). Figure 2C shows the inner surface of the pockets. In group I mice (ADSCs mixed with minced adipose tissue implanted), a reddish and richly vascularized pocket was formed in the subcutaneous tissue. However, vascularization was poor in the tissue pockets of mice in groups II (ADSCs implanted only), III (minced adipose tissues implanted only), and IV (nothing implanted as control).

The subcutaneous space of recipient mice preimplanted with ADSCs and/or adipose tissue was examined histologically (Fig. 2D, E). Group I recipient mice showed a grafted adipose tissue layer in the subcutaneous space (Fig. 2D). The removed spacer had clearly passed through the center of the

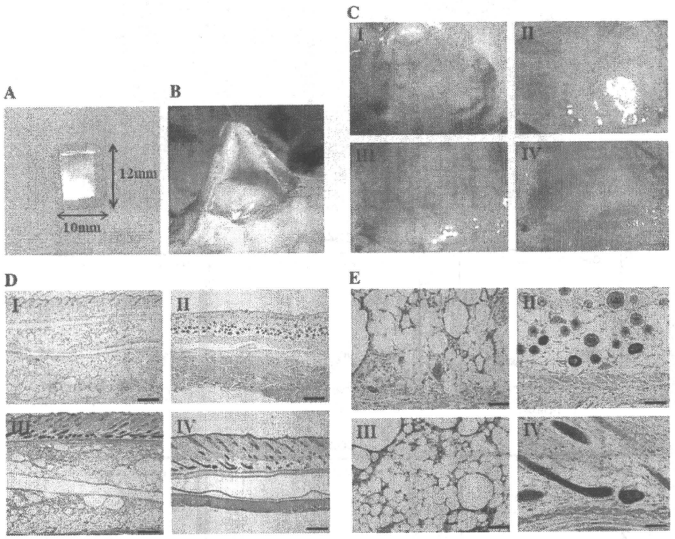


FIG. 2. Pocket creation for subcutaneous transplantation of islets. (**A**) Polyester spacer inserted into the back of mice. The material of the temporarily implanted spacer was nonbiodegradable and non-cell-adherent because the spacer needs to be removed before implantation of islets. (**B**) The pocket for islet transplantation. After removal of the spacer at 4 weeks after surgery, a pocket was formed in the subcutaneous tissue into which islets could be easily transplanted. (**C**) Macroscopic examination of the subcutaneous pocket. Rich vascular networks were apparent in group I mice, implanted with ADSCs mixed with minced adipose tissue. The vascular network was poorly formed macroscopically in all other groups. (**D**) Histological examination of the pretreated subcutaneous tissue (hematoxylin and eosin staining). Bars indicate 500 μm. (**E**) High-power micrographs. Abundant vessel-like structures were observed in group I mice (mixture of ADSCs and minced adipose tissue). Group II (ADSCs only) mice tissue showed some vessels around a capsule in the subcutaneous tissue. Group III (minced adipose tissue only) and group IV (nothing implanted) showed poor vascular modification than group I. Bars indicate 100 μm.

grafted adipose tissue. Tissue sections from group I mice also showed an abundant vessel structure filled with red blood cells, while this was not seen in mice from the other three groups (Fig. 2E). Recipient mice from group III had a similar grafted adipose tissue layer to group I mice, but the vascular formation was poor. Mice from group II showed some vessel-like structures around a capsule in the subcutaneous tissues, and a few vessels were observed histologically in group IV mice.

*Evaluation of vascular beds in the transplantation pocket*

To evaluate vascular bed formation in the pocket, sections of subcutaneous tissues from mice of groups I–IV were stained for von Willebrand factor (Fig. 3A) to visualize such vessels. Vascularization was evaluated by the vessel number per square millimeter of subcutaneous tissue harvested at 4 weeks after implantation (Fig. 3B). The number of detectable

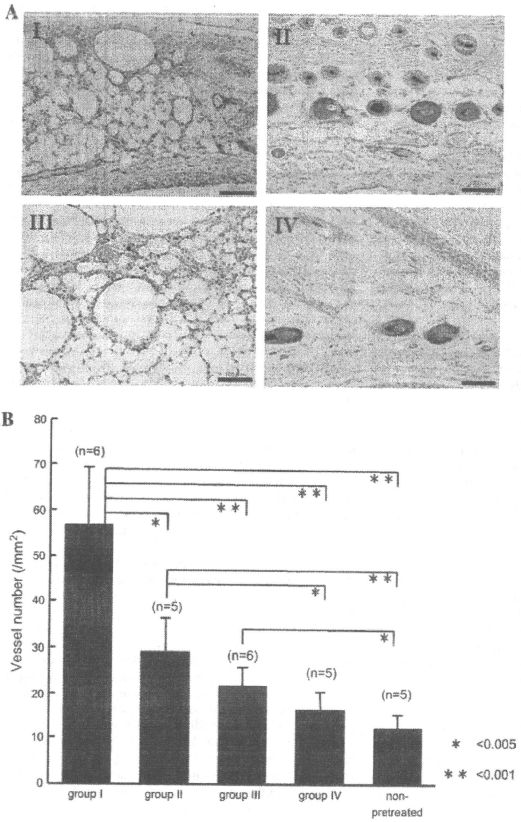


FIG. 3. Evaluation of vascular networks in the subcutaneous pockets. (**A**) Immunostaining for vWF to visualize the vasculature of subcutaneous tissue surrounding the pockets. Group I mice (mixture of ADSCs and minced adipose tissue implanted) showed more vessels than all other recipient mice. Bars indicate 100 μm. (**B**) Vascular network evaluation by vessel number. Vessels per square millimeter in the implanted subcutaneous tissue were counted at 4 weeks after building of the pockets. vWF-positive tubule-like structures were counted as vessels. Group I mice showed a significant increase in vessel number compared with all other groups. Values are means ± S.D. *$p < 0.05$; **$p < 0.01$.

vessels in group I mice was significantly higher than in those from all other groups (group I, $57 \pm 12/mm^2$; group II, $29 \pm 7/mm^2$; group III, $21 \pm 4/mm^2$; group IV, $16 \pm 4/mm^2$; nonpretreated control mice, $12 \pm 3/mm^2$). The density of these vessels was higher in groups II and III than that in nonpretreated control mice, although not to the extent of group I. There was no significant difference in vessel number between group IV mice (spacer only inserted) and nontreatment control mice, indicating that the spacer had no effect on vascularization. These results indicate that implantation of a mixture of ADSCs and minced adipose tissue is the most promising for vascular bed formation before islet transplantation.

### *Islet transplantation into the vascular-modified subcutaneous pockets*

To examine whether the subcutaneous tissue pockets could support functional islet transplantation, nonfasting blood glucose levels of recipient mice after transplantation
F4 ▶ were determined serially (Fig. 4A). All recipient mice of group I (implanted mixture of ADSCs and minced adipose tissue; $n = 7$) showed a rapid decrease in blood glucose level to normoglycemia (<200 mg/dL) within 1 week after islet transplantation, and the normoglycemia was maintained for over 8 weeks. These mice became hyperglycemia again after removal of the subcutaneous graft. The nonfasting blood levels decreased slightly after islet transplantation in group II mice ($n = 7$), but not to normoglycemic levels. No recipient mice of group III ($n = 5$) or group IV ($n = 5$) showed a decrease in nonfasting blood glucose levels during the 8-week posttransplantation period.

Intraperitoneal glucose tolerance tests were performed for recipient mice of group I at 3 weeks after islet transplantation (Fig. 4B). All mice in this group showed a good response to the glucose load with an immediate return to normoglycemia, as observed in nondiabetic mice.

Many viable islets were detected in the grafted adipose tissue of group I mice at 8 weeks after islet transplantation (Fig. 4C). Immunohistochemical examination revealed that the engrafted islets could also produce insulin *in vivo* over the longer term (Fig. 4C, right panel), indicating that the grafted islets received sufficient oxygen and nourishment via the neovascularization for adequate function in the subcutaneous tissue.

## Discussion

Subcutaneous tissue was proposed as an optimal site for therapeutic islet transplantation based on easy access for implantation and removal of the graft with minimal invasiveness. However, unmodified subcutaneous tissue lacks the blood flow needed to support the transplanted islet in a functional state, leading to graft ischemia and necrosis. It is thus necessary to establish dense vascular networks to sufficiently nourish the transplanted grafts and maintain long-term function. We have established a technique to prepare vascular beds in subcutaneous tissue suitable for a transplant site by preimplanting a combination of ADSCs and minced adipose tissue.

Previous studies subcutaneously implanted artificial devices containing basic fibroblast growth factor (bFGF) or matrigel, with a pored stainless steel diffusion chamber serving as the vascularizing device.[10–13] The grafted islets in these cases showed functional insulin production at the subcutaneous tissue sites.[10–13] However, long-term placement of artificial material in the body may cause overgrowth of fibroblasts and calcification surrounding the device due to chronic inflammation, leading to a diminished supply of oxygen and nutrition to the transplanted graft.[21] Our method avoids these problems by using the patient's own tissues, thus making it more attractive for clinical application.

A previous study demonstrated vascularization followed by reperfusion of blood flow to ischemic sites when ADSCs were implanted in ischemic model animals.[22] The vascularization effects of ADSCs probably depend on the following two mechanisms. First, ADSCs secrete angiogenic growth factors such as hepatocyte growth factor and vascular endothelial growth factor (VEGF).[22,23] Second, ADSCs can themselves differentiate into endothelial cells to make new vessels.[14,15] Further, ADSCs augment the secretion of angiogenic growth factors such as VEGF under hypoxic conditions.[23]

In the present study, dense vascular networks were induced in the subcutaneously grafted adipose tissue in recipient mice implanted with a mixture of ADSCs and minced adipose tissues. In addition, the density of capillary vessels in the subcutaneous tissue was significantly higher in these mice than in the other experimentally implanted or nonimplanted mice. We propose the following mechanisms for the improved vascularization with a mixture of stem cells and adipose tissue over either of the components implanted alone. First, mixing ADSCs with the adipose tissue stimulates an artificial hypoxic state, setting off a signaling cascade from the adipose tissue to the ADSCs to respond to the ischemia by vascularization. In addition, the adipose tissue forms an ideal scaffold for the ADSCs to engraft and function in subcutaneous tissue.

The vascular beds in subcutaneous tissue prepared by our method supplied sufficient blood flow to the engrafted mouse islets for successful long-term engraftment and function. The results of intraperitoneal glucose tolerance tests indicated that the grafted islets functioned similar to normal islets in nondiabetic mice, and that all recipient mice became hyperglycemic again after removal of the graft-bearing subcutaneous tissues. These data confirmed that the transplanted islets were functional and able to correct the blood glucose levels of the diabetic recipient mice. Our study therefore showed for the first time that the rich vascular beds needed for transplantation were successfully induced in normal subcutaneous tissue by ADSCs.

In another similar article, Chen *et al.* reported that the intraabdominal epididymal fat pad had high blood flow and was a useful site for islet transplantation as well as the liver via portal vein in a mouse model.[24] However, their technique is a invasive procedure for the recipient, because a laparotomy under general anesthesia is necessary. At the same report, they said that the epididymal fat may not be a practical site for clinical islet transplantation. Although the subcutaneous tissue has insufficient blood flow, the clinical application of subcutaneous islet transplantation is possible enough by adding pretreatment. Considering the relationship of the skin surface area and implanted islet volume, we

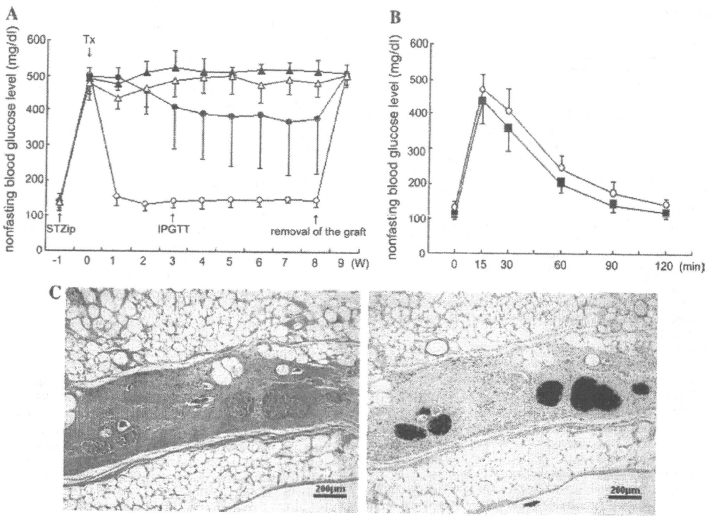


4C ▶

**FIG. 4.** Vascular network–formed subcutaneous pockets are suitable sites for islet transplantation. **(A)** Nonfasting blood glucose levels in each group of recipient mice after islet transplantation. All group I recipient mice (mixture of ADSCs and minced adipose tissue implanted) showed a rapid decrease in blood glucose level to normoglycemia (<200 mg/dL) within 1 week after islet transplantation; this was maintained for over 8 weeks. These mice became hyperglycemic again after removal of the subcutaneous grafts. Open circles, group I ($n=7$); closed circles, group II ($n=7$); open triangles, group III ($n=5$); closed triangles, group IV ($n=5$). Error bars indicate SD. **(B)** Intraperitoneal glucose tolerance test was performed on recipient mice of group I (mixture of ADSCs and minced adipose tissue implanted) at 3 weeks after islet transplantation and on nondiabetic mice. Group I mice (open circles, $n=5$) showed a good response to the glucose load, immediately returning to normoglycemia in a manner similar to nondiabetic mice (closed squares, $n=5$). Error bars indicate SD. **(C)** Histological examination of the grafted islet–bearing subcutaneous tissue. Many viable islets were found in the grafted adipose tissue resected from recipient mice in group I at 8 weeks after islet transplantation (left panel, hematoxylin and eosin staining). All grafted islets were immunohistochemically positive for insulin (right panel). Bars indicate 200 μm.

think that approximately 400,000 human islets are able to be transplanted in an area of 10 $cm^2$.

Regenerative medicine for diabetes is an emerging area for potential clinical application, and administration of these transdifferentiated insulin-producing cells looks promising as a novel therapy.[25,26] For realization of stem cell–derived cellular therapy, the transdifferentiated cells should not elicit adverse events such as carcinogenesis or infection. One big advantage of our method is that if such complications occur after administration, the grafts could be removed relatively easily in comparison to conventional islet transplantation procedures.

In conclusion, we successfully established rich vascular networks in subcutaneous tissue using the recipient's own bioresources, that is, ADSCs and subcutaneously derived adipose tissue. Islets implanted into these vascularized sites engrafted successfully and functioned well in the subcutaneous tissue over a long term. Our study promises the potential of islet transplant therapy and a future platform for cell-based treatment of diabetes involving regenerated insulin-producing cells.

### Acknowledgments

This study was supported in part by a Grant-in-Aid to Yoshiki Sawa from New Energy and Industrial Technology Development Organization (NEDO), Japan, and in part by a Grant-in-Aid to Akifumi Matsuyama from Kobe Translational Research Cluster, the Knowledge Cluster Initiative, Ministry of Education, Culture, Sports, Science and Technology (MEXT), Japan.

### Disclosure Statement ◀ AU2

No competing financial interests exist.